BULLETIN OF THE CHEMICAL SOCIETY OF JAPAN VOL. 41 479—485 (1968)

The Zinc Oxide-Copper Catalyst for Carbon Monoxide-Shift Conversion. II. The Catalytic Activity and the Catalyst Structures

Hiroshi UCHIDA,*1 Masaaki OBA, Norio ISOGAI*2 and Toji HASEGAWA

Government Chemical Industrial Research Institute, Tokyo, Shibuya-ku, Tokyo

(Received August 28, 1967)

Structures of the zinc oxide-copper catalysts, whose catalytic activity in carbon monoxide-shift conversion had been determined, were investigated by X-ray diffraction technique, mercury- and helium-volume measurement, and electron microscopy. The electron microscopic observations were conducted in two ways; one on a catalyst sample after the activity test and the other on a raw sample while undergoing specified treatments in a reaction chamber attached to the electron microscope. On the basis of models of particle geometry obtained from the electron microscopic images, the results on pore volume, average diameters of pores and particles, all dependent on the method of preparation and the chemical composition, are explained. The models and the observed dependency of the specific activity of copper surface on the copper content indicate that the finer copper particles, whether patch-like or massive, show the higher specific activity. The fine copper particle is apt to be oxidized more readily than the well-grown particle.

The preceding paper[1] described how the preparation method and the chemical composition of zinc oxide-copper catalysts are related to their catalytic activity in carbon monoxide-shift conversion. The catalysts studied were a series of catalysts of varying copper contents prepared by kneading zinc oxide powder with copper hydroxide cake (the kneaded series) and a couple of catalysts of an approximate copper content prepared by the impregnation and the coprecipitation method. Practicable catalysts could be produced only by the kneading process provided they contained appropriate amounts of copper. As regards the kneaded series, a model of particle geometry that copper forms its own particles among the original zinc oxide powders was tentatively proposed and successful in an attempt of explaining the observed dependency of catalytic activity on the chemical composition, but exact knowledge on structures of the catalysts is still lacking. In the present study, the catalyst structures will be investigated, the results of which may be used for an understanding of the catalytic activity from the structural viewpoint of the catalysts.

Experimental

Table 1 presents the method of preparation and the chemical composition of catalysts repeatedly. Experimental methods used for investigating catalyst structures include X-ray diffraction technique, mercury- and helium-displacement method, and electron microscopy.

The X-ray diffraction diagram for a powdered sample of the catalyst was obtained with an X-ray diffractometer of the Geigerflex D-3F type. The nickel filtered Cu$K\alpha$ radiation from a sealed-off tube with berylium windows was used. The tube was operated at 40 kV and 18 mA. The volumes by the mercury- and helium-displacement method were determined on catalyst grains after they had been used in the activity test for carbon monoxide-shift conversion.

TABLE 1. METHOD OF PREPARATION AND CHEMICAL COMPOSITION OF CATALYSTS

Catalyst No.	Method of preparation	Cu/Zn atomic ratio
1	Kneading[a]	ZnO
2	Kneading[a]	0.09
3	Kneading[a]	0.25
4	Kneading[a]	0.45
5	Kneading[a]	0.68
6	Kneading[a]	0.90
7	Kneading[a]	1.98
8	Kneading[a]	2.95
9	Kneading[a]	9.70
10	Kneading[a]	Cu
21	Impregnation	0.34
22	Coprecipitation	0.40

a) Zinc oxide powder was kneaded with a copper hydroxide cake into a pasty mixture, which was dried at 150°C, pelleted, and heat-treated in the air at 250°C. A series of catalysts 1—10 with be designated as the kneaded series.

*1 Present address: Faculty of Engineering, Nagoya University, Chikusa-ku, Nagoya.

*2 Present address: Japan Gas Chemical Co., Enoki-cho, Niigata.

1) H. Uchida, N. Isogai, M. Oba and T. Hasegawa, This Bulletin, **40**, 1981 (1967).

The size and shape of particles of a catalyst sample after the activity test were examined under an electron microscope of the JEM-6A type. Moreover, changes in shape of particles were pursued under the electron microscope on a dried paste (the sample after drying at 150°C a pasty mixture of oxide or hydroxide of zinc and copper hydroxide) while the paste was undergoing such treatments as heating in the air and subsequent reduction in hydrogen. In particular cases, the paste was oxidized finally in the air. These treatments were conducted in a reaction chamber attached to the electron microscope.

The reaction chamber is schematically drawn in Figs. 1A and 1B. The chamber is a stainless steel cylinder (C) (110 mm diameter by 100 mm long) and attached to the electron microscope by way of an air-lock (L). It is equipped with two valves, one (V) for introduction of a reactant gas (hydrogen or air) at a constant feed rate (10 *l*/hr) at atmospheric pressure and another (V') either for withdrawal of the gas at atmospheric pressure or for evacuation. A holding device (A, for details see Fig. 1B showing another side of 1A) of a sample is centrally held in the chamber by means of a perforated stainless steel rod (R) inserted from top of the chamber. Through the perforation pass an insulated Pt-Pt·Rh thermocouple and two insulated nichrome wires leading to a nichrome wire heater (I). A stainless steel sample holder (H), which is similar in dimension to the one as conventional in the electron microscopic observation and which has small ceramic protruding parts around its supporting drim, is mounted vertically in a notched steatite cylinder having a steatite drim (J). The nichrome wire heater (I) is wound along the notch. The steatite drim is fixed to the rod (R) one over another together with a stainless steel plate (K), into which a stainless steel tube for protection of the heater is screwed. A horizontally movable rod (M) with a fork at the end carries the sample holder, while the holder being hung by the ceramic protruding parts, into and out of the electron microscope through the air-lock open.*3

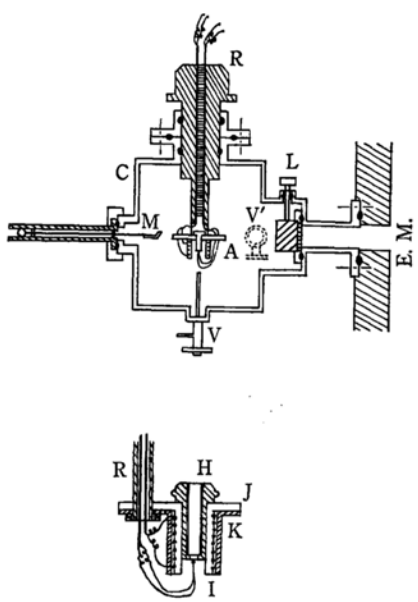

Fig. 1. Schematic diagram of reaction chamber.
Above: Fig. 1A, below: Fig. 1B

The sample was ground in a mortar to powder. The powder was sprinkled by means of an adsorbent cotton over an evaporated silica film supported on a stainless steel mesh, which was then placed at bottom in the sample holder. The temperature at which the sample was undergoing progressive reduction processes in hydrogen or oxidation in the air was measured with the Pt-Pt·Rh thermocouple just below the mesh. The electron microscopic observations were conducted at time intervals after the successive treatments of a short period.

Results

The X-Ray Diffraction Diagram. The raw copper hydroxide cake gave a complicated diffraction diagram, indicating the presence of basic copper hydroxide, $Cu_2(OH)_3(NO_3)$, in addition to that of copper hydroxide. However, no more sign other than oxides of copper and zinc appeared in the diagram of the finished sample.*4 This reveals rapid decomposition of both the basic hydroxide and the hydroxide into the oxide by a simple heat-treatment in the air at 250°C. After having been used in the activity test, all the samples including catalysts 21 (the impregnated catalyst) and 22 (the coprecipitated catalyst) gave sharp diffraction lines due to zinc oxide and copper in addition to very weak and diffused lines due to copper oxide (*e. g.* Ref. Fig. 2 for catalyst 4). Lattice constants of the zinc oxide were found to be $a=3.255$—3.285 Å and $c=1.60$ Å, while the constant of copper $a=3.618$—3.628 Å, the values being identical with the literature values.

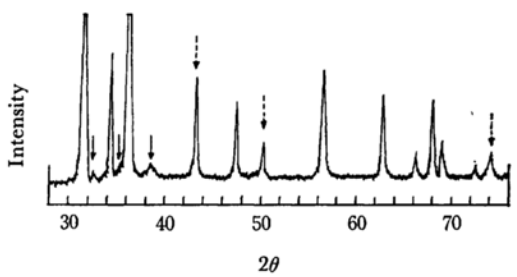

Fig. 2. X-Ray diffraction diagram of catalyst 4 after use in activity test.
The arrows indicate the lines due to copper oxide.

The Total Pore Volume and the Porosity. The mercury-volume and the helium-volume (hereafter denoted by V_{Hg} and V_{He} respectively) of catalyst grains are presented in Fig. 3 as a function of the catalyst chemical composition expressed

*3 Details of procedures for the observation will be described elsewhere.

*4 Refer to the foot note of Table 1.

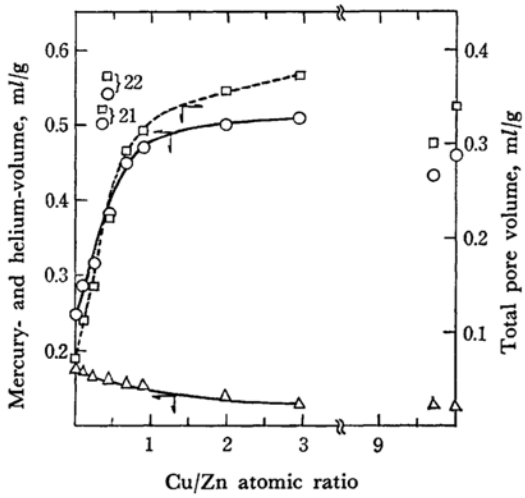

Fig. 3. Mercury- and helium-volume and total pore volume as function of Cu/Zn atomic ratio.
○: V_{Hg}, △: V_{He}, □: V_{po}

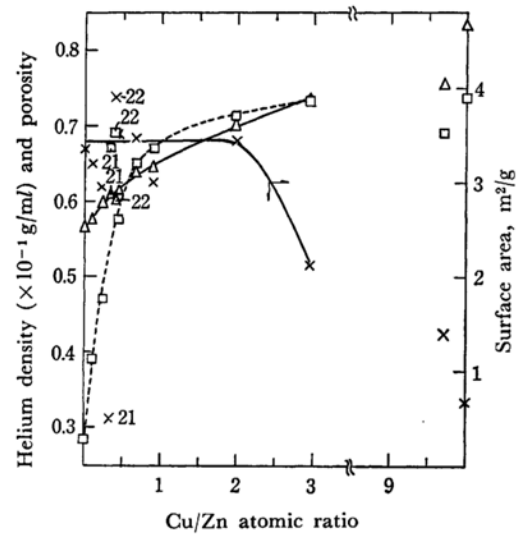

Fig. 4. Helium-density, porosity, and specific surface area plotted against Cu/Zn atomic ratio.
□: porosity, △: ρ_t, ×: S

by the Cu/Zn atomic ratio. The total pore volume (V_{po}) was then obtained as the difference between V_{Hg} and V_{He}, while the porosity (θ) as the ratio of V_{po} to V_{Hg}. The V_{po} and the θ are plotted in Figs. 3 and 4 against the Cu/Zn atomic ratio respectively. These two plots similarly rise rapidly with the ratio in the initial range below 1, less steeply in the intermediate range. In the final range of high ratios (probably >5), the V_{po} turns to fall, whereas the θ remains almost constant. The V_{po} values of catalysts 21 and 22 are much larger than those of catalyst 4, the corresponding catalyst (the catalyst approximate in copper content) of the kneaded series.

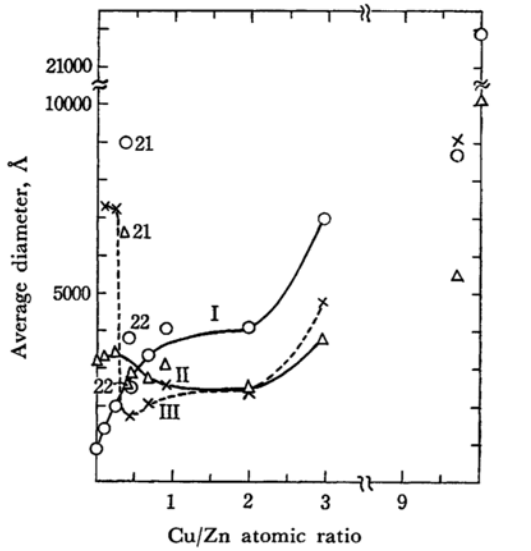

Fig. 5. Average diameters of pores and particles as function of Cu/Zn atomic ratio.
○ (I): $\bar{d}_{po}$, △ (II): $\bar{d}_{pa}$, × (IIII): $\bar{d}_{paCu}$ calculated on the basis of model II in the preceding paper.

The Average Diameter of Pores and Particles. On the assumption of cylindrical pores the average pore diameter ($\bar{d}_{po}$) was claculated by the equation of $\bar{d}_{po}=4V_{po}/S$, where S was the specific surface area of catalyst, on the assumption of spherical or cubic particles the average particle diameter ($\bar{d}_{po}$) was calculated by the equation of $\bar{d}_{pa}=6/\rho_t S$, where ρ_t was the true density or $1/V_{He}$ (Ref. the plot in Fig. 4). Plots of the $\bar{d}_{po}$ and the $\bar{d}_{pa}$ against the Cu/Zn atomic ratio are shown in Fig. 5 (the plots I and II respectively). As the copper content increases, an initial rapid rise in the plot of $\bar{d}_{po}$ is followed with a slower rise. In contrast, the plot of $\bar{d}_{pa}$ first rises very slowly, turns to fall at a ratio of *ca.* 0.3, and finally rises again after passing through a minimum at a ratio of 2.0. For both of these plots, the rises in the range of very high ratios seem not so rapid.

The $\bar{d}_{po}$ and $\bar{d}_{pa}$ values of catalysts 21 and 22 do not fit the respective plots of the kneaded series; as compared with catalyst 4, these two catalysts show the $\bar{d}_{po}$ values somewhat large, but the $\bar{d}_{pa}$ value is slightly small for catalyst 22 and considerably large for catalyst 21.

The Electron Microscopic Image. Figure 6-(a) presents an electron micrograph of powders of the raw zinc oxide, while electron micrographs of catalysts 2, 4, and 8 after the activity test are shown in (b), (c), and (d), of the same figure respectively. On these latter micrographs, it is difficult to immediately distinguish between zinc oxide

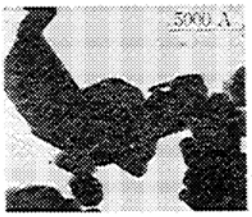

(a) Cat. 1 (ZnO)

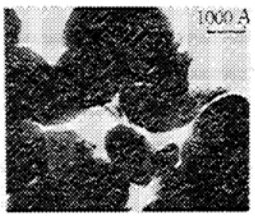

(b) Cat. 2 (Cu/Zn=0.09) after use in activity test

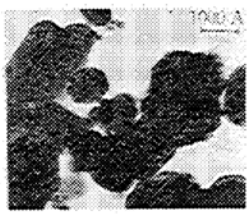

(c) Cat. 4 (Cu/Zn=0.45) after use in activity test

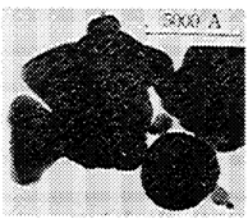

(d) Cat. 8 (Cu/Zu=2.95) after use in activity test

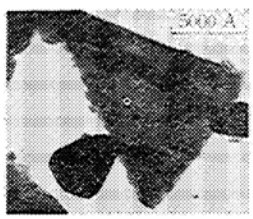

(e) Cat. 8 (Cu/Zn=2.95), dried paste

(f) Cat. 8, after heating of sample of (e) in air at 250°C for 5 min

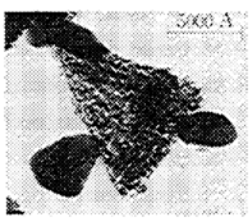

(g) Cat. 8, after reduction of sample (f) in H_2 at 180°C for 5 min

(h) Cat. 8, after further reduction of sample of (g) in H_2 at 350°C for 5 min

(i) Cat. 8, after oxidation of sample of (h) in air at 200°C for 2 min

(j) Cat 21 (impregnated cat., Cu/Zn=0.34), after heating dried sample in air at 250°C for 5 min

(k) Cat. 21 after reduction of sample of (j) in H_2 at 250°C for 5 min and at 400°C for 5 min

(l) Cat. 22 (coprecipitated cat., Cu/Zn=0.40), after heating dried sample in air at 250°C for 5 min

(m) Cat. 22 after reduction of sample of (l) in H_2 at 250°C for 5 min at 400°C for 5 min

Fig. 6. Electron micrographs [(a)—(m)].

and copper, but further insight into this can be obtained by refering to a series of micrographs (e)-(h), which illustrate changes in size and shape of both a copper hydroxide particle and a zinc oxide powder of a dried paste (the paste for preparation of catalyst 8) while the paste is under going the specific treatments in the reaction chamber.

In contrast to the pracitcally non-porous zinc oxide powder of distinct contour, the copper hydroxide particle in the dried paste is characterized by its thin plate-like structure of a comparatively large dimension [Ref. (e)]; a part of this plate seems to have been torn into pieces, which lie on the surface of the zinc oxide powder. On heating at 250°C, the plate-like particle shrinks a little with simultaneous production of a large number of extremely fine copper oxide particles within [Ref. (f)]. When reduced with hydrogen at 180°C for a short period, these fine particles exhibit considerable mobility and grow to irregularly shaped particles of several hunderd Å in width [Ref. (g), conveniently designated as the primary particles hereafter]. On futher reduction at a higher temperature of 350°C, large majority of these primary particles stick together to form a plate-like aggregate (the secondary particle) of copper occupying a slightly smaller area than before, while a part of them is left behind along periphery of the previous plate-like particle [Ref. (h)]. This aggregate is rather inhomogeneous in structure. Meanwhile, the pieces of copper oxide having lied on the surface of a zinc oxide powder are reduced *in situ* to form patches of copper. It should be emphasized that the primary particles of copper do not tend to stick to the zinc oxide powder. The zinc oxide powder preserves its size and shape throughout these treatments, and this is also true even for the catalyst smaple after the activity test [Ref. (b) and (c)].

On the basis of information available on a series of micrographs (e)-(h), it is possible to state that the particle image with an obscure contour in the series (b)-(d) represents a copper particle. It has appeared, accordingly, that copper in the sample after the activity test often forms, in addition to its massive particles, its thin, small flakes lying flat on the surface of zinc oxide powder. This is particularly the case with catalysts containing relatively small amounts of copper [Ref. (b) and (c)]; as the copper content is increased progressively, the massive particles increase in number at the expense of the thin flakes, insofar as the copper content remains within a certain limit [compare (b) with (c)]. However, matters are different for catalyst 8 of a high copper content [Ref. (d)]; the zinc oxide powder in the sample after the activity test is seemingly covered, at least partially, with layers of copper and frequently a few of these powders collect together to form an irregularly shaped, much larger aggregate [Ref. (d)].

The electron micrographs of catalysts 21 and 22 after the activity test appear quite different from that of catalyst 4; the particle is as large as that of catalyst 4, but shows too homogeneous a structure to permit a distinction to be made between zinc oxide and copper.*5 Although the original zinc oxide powder is not at all disintegrated by having been kneaded with a copper hydroxide cake, the powder is disintegrated at some depth from periphery by impregnation with a copper nitrate solution [Ref. (j)], and copper produced by reduction in this region is disperesed homogeneously in zinc oxide [Ref. (k)]. With catalyst 22, mutual dispersion between the two components is finer in degree than with catalyst 21, before as well as after reduction [Ref. (l) and (m), and also compare (m) with (k)]. The pronounced particle growth taking place with these two catalysts during the activity test may perhaps be due to a some less stable structure of the particles, but nothing more decisive can be said.

Upon oxidation with air at 200°C for a short period, the copper aggreagte (the secondary particle) in (h) for catalyst 8 is readily back in size and shape to the previous aggregate in (g). No trasformation of this kind, however, was observed for such a well grown copper particle with a smoothed, sharply outlined contour of the same catalyst as shown in (d), even though the particle had been oxidized at a higher temperature of 300°C.*5 These findings reveal that the secondary particle which is an aggregate of the small primary particles with uneven surfaces is oxidized more easily than the massive, large particle with a smoothed surface.

Discussion

The Total Pore Volume and the Average Pore Diameter. In the light of the results of the electron microscopic observations, an attempt will be here made to explain the trends in the changes of V_{po} and $\bar{d}_{po}$ with the copper content for the catalysts of the kneaded series (Ref. Fig. 3 and the plot I in Fig. 5 respectively). If the catalyst contains not so large a amount of copper, the greater part of copper exists, immediately after reduction, as the plate-like aggregates among the zinc oxide powders, and each of these aggreagates transforms *in situ*, with shrinking, to a massive particle after the catalysts have been used in the activity test, whereas each of the original zinc oxide powders remains unaltered in size and shape. Accordingly, the larger the copper content is the larger is the V_{po}, which has been produced within original matrix of zinc oxide powders by the shrinking of aggreagates. Since the $\bar{d}_{po}$ is related to the V_{po} through the equation of $\bar{d}_{po}=4V_{po}/S$,

*5 The electron micrograph is not presented here in order to reduce number of micrographs.

the $\bar{d}_{po}$ is to change in the same way as the V_{po} does if the S differes little with copper content. This is, in fact, the case with this series of catalysts (Ref. the plot I in Fig. 4). If the catalyst, however, contains a very large amount of copper, the zinc oxide powder becomes covered with layers of copper after the activity test and, as a consequence, more easily sinter with each other to grow to large aggregates. This results in the V_{po} decreasing with the copper content (Ref. Fig. 3). In spite of this decrease in the V_{po}, the $\bar{d}_{po}$ in this range still decreases, which fact may come from the S decreasing more rapidly with the copper content (Ref. the plot in Fig. 4) than the V_{po}.

The abnormally high V_{po} values of catalyst 21 and 22, as compared with that of catalyst 4, can not be explained on the basis of the results of electron microscopic observations alone. This may perhaps be ascribed to the difficulty in finishing the raw paste to pellets as dense as those of the kneaded series.

The Average Particle Diameter. The previous particle model (model II in the preceding paper[1]) by no means accounts for the initial slow rise in the plot of $\bar{d}_{pa}$ (Ref. the plot II in Fig. 5). The model was conveniently proposed in order to explain the change in the specific activity of copper surface with varying copper contents, and it was assumed that, for every catalyst studied, particles consisting of copper alone were distributed among the original zinc oxide powders. However, the previous model has proved to agree only incompletely with the models of particle geometry presented in this paper. Provided the catalysts contain not a very large amount of copper, portion of copper exists as patches on the surface of zinc oxide powder, while another portion as massive particles. According to this model, the copper added is to contribute for enlarging the $\bar{d}_{pa}$ rather than reducing it, which is justified with the initial rise in the plot. In the range of moderate copper contents, the previous model has proved to be almost true; the $\bar{d}_{pa}$ is then likely to decrease as the copper content is increased, because the copper particles, which are small in size as compared with the zinc oxide powders, increase in number. The previous model differs again in the range of sufficiently large copper contents; the original zinc oxide powder is covered with layers of copper. This may bring about easier particle growth by agglomeration, and hence a rise in the plot of $\bar{d}_{pa}$. Neither the previous model fails to explain this rise, but the present explanation, being based on a more concrete model, is preferable.

In the preceding paper,[1] the surface area of copper per 1 g of catalyst, S_{Cu}, was calculated on the basis of the previous model. However, this model has proved to agree with the electron microscopic images only for the catalysts of moderate copper contents, and the S_{Cu} values might, in general, have been subject to considerable error except for the above-stated catalysts. In fact, calculation of the average diameter, $\bar{d}_{paCu}$, of copper particles by $\bar{d}_{paCu}=6/S_{Cu}\rho_{Cu}$ (ρ_{Cu}, the copper density=8.92) using the previous S_{Cu} values results in unreasonably large values with the catalysts of a very small copper content (Ref. the plot III in Fig. 5). The previously calculated values of S_{Cu} must have been underestimated for any of the catalysts containing either a very small or a very large amount of copper, because the calculation of S_{Cu} for this was conducted without consideration of the copper surface area due to patches or layers of copper on a zinc oxide powder. Unfortunately, it is difficult, however, to evaluate accurate extents of adjustment from the data available.

The Structure of Copper Responsible for the High Specific Activity. In the preceding paper,[1] the specific activity of copper surface (the activity per unit of area of the copper surface) at a reaction temperature, *e. g.*, of 180°C, k'_{Cu180}, was obtained by the equation of $k'_{Cu180}=k_{180}/\rho_b S_{Cu}$, where k_{180} was the rate constant*6 at 180°C per unit of volume of the catalyst bed, and ρ_b is the catalyst bed density, on the reasonable assumption that only the copper surface is effective in the reaction. The k'_{Cu180} values obtained by the use of the previous S_{Cu} values were very high in the range of very small copper contents, fell rapidly and then gradually with the copper content.[1] In this connection, the k'_{Cu180} values in each of the two extreme ranges of either very small (the lower range) or very large copper contents (the upper range) should be more or less reduced from the previous values owing to the k'_{Cu} values having been underestimated, whereas the values in the range between these extremes (the intermediate range, 0.4—2.0 in the Cu/Zn atomic ratio) are to vary little from the previous values. Nevertheless, the decreasing trend of k'_{Cu180} with the copper content is likely to be retained, though only qualitatively, over the whole range studied; even though the k'_{Cu180} value in the two extreme ranges is reduced, the decreasing trend of the k'_{Cu180} with the copper content in the upper range is not affected substantially and at the same time any downward bend is scarcely suspected with the plot of the k'_{Cu180} rising with the decreasing copper content in the lower range, where the activation energy of reaction is lowering with the decreasing copper content.[1] This and the present models of particle geometry indicate that the finer copper particles, whether patch-like or massive, are responsible in structure for the higher specific activity.

*6 The k was calculated by the aid of the rate equation of Kul'kova-Temkin.[2]

Taking into account the finding that the finer copper particles are oxidized more easily, it may be concluded that the copper surface participates in the reaction to the extent that the surface is apt to be oxidized. This may lend another support, though not directly, to the view of Temkin *et al.*[2,3] on the reaction rate over an iron oxide, who proposed a mechanism according to which the gaseous components react with oxidized and reduced surface sites as expressed by the following scheme:

$$CO + (O) = CO_2 + (\ )$$

$$H_2O + (\ ) = H_2 + (O)$$

where ( ) and (O) designate reduced and oxidized site respectively.

The poor and unstable activity, in spite of the mutual dispersion between zinc oxide and copper, of catalysts 21 and 22 is explained only with difficulty. A probable explanation for this may be that too fine a dispersion, in turn, causes copper to be included into interior of the particle and a small extent of copper becomes available on the particle surface.

2) N. V. Kul'kova and M. I. Temkin, *Zhur. Fiz. Khim.*, **23**, 695 (1949).

3) G. G. Shchibria, N. M. Morozov and M. I. Temkin, *Kinetika i Kataliz*, **6**, 1057 (1965).